The Complex Behaviour of a Simple Neural Oscillator Model in the Human Cortex

Pavel Cejnar, Oldřich Vyšata, *Member, IEEE*, Martin Vališ, and Aleš Procházka, *Senior Member, IEEE*

***Abstract*— The brain is a complex organ responsible for memory storage and reasoning; however, the mechanisms underlying these processes remain unknown. This paper forms a contribution to a lot of theoretical studies devoted to regular or chaotic oscillations of interconnected neurons assuming that the smallest information unit in the brain is not a neuron but, instead, a coupling of inhibitory and excitatory neurons forming a simple oscillator. Several coefficients of variation for peak intervals and correlation coefficients for peak interval histograms are evaluated and the sensitivity of such oscillator units is tested to changes in initial membrane potentials, interconnection signal delays, and changes in synaptic weights based on known histologically verified neuron couplings. Results present only a low dependence of oscillation patterns to changes in initial membrane potentials or interconnection signal delays in comparison to a strong sensitivity to changes in synaptic weights showing the stability and robustness of encoded oscillating patterns to signal outages or remoteness of interconnected neurons. Presented simulations prove that the selected neuronal couplings are able to produce a variety of different behavioural patterns, with periodicity ranging from milliseconds to thousands of milliseconds between the spikes. Many detected different intrinsic frequencies then support the idea of possibly large informational capacity of such memory units.**

***Index Terms*— Brain activity modelling, neural oscillators, knowledge representation, Izhikevich neuron model, spiking neural networks, signal processing.**

I. Introduction

MANY theories regarding processes responsible for memory storage and reasoning in the brain exist, often based upon neurotransmission [1]–[4], however the underlying mechanisms of these processes remain still generally unknown. Computer artificial neural networks are also originally based on observations and assumptions about these brain processes [5]. Biological neural networks, including the human brain, are characterized by continuous oscillatory activity. This oscillatory activity is generally considered to be slightly chaotic, but low-level chaos is absent [6]. The biological significance and mechanisms of this activity are unknown. Some researchers attribute oscillatory activity to the noise that accompanies information processing in neurons [7], other hypothesis interprets brain oscillations as a phenomenon of synchronization of oscillatory activity [8], [9]. Investigating the mechanisms of learning at neuronal circuit level is technologically very demanding and includes monitoring the behavioural dynamics of these neuronal circuits. The mechanisms underlying knowledge representation in brain are still generally poorly known. It has been shown that even primitive organisms, like *Caenorhabditis elegans* with approximately 300 neurons only, are equipped with some basic memory capabilities [10], [11]. And thus the long- and short-term memory function in human brains is thought to be embedded in the neuron/synapse structure. In theory even two excitatory and one inhibitory neurons when properly interconnected could form a chaotic oscilator [12], [13]. If we accept the hypothesis that the smallest information-processing unit is not a neuron alone but, instead, a neural oscillator composed from excitatory and inhibitory interneurons and their interconnections for the resulting oscillatory activity, such a model is also fully compatible with current models of the latest (the third) generation of artificial computer neural networks, so called spiking neural networks.

A lot of theoretical work has been done regarding capability of modelled neurons to produce regular or chaotic oscillations [8], [13], however even basic studies about stability of such knowledge representation are still missing. For this reason we present here a study of sensitivity of such knowledge representation to changes in several well-explained parameters. If we accept the idea of encoding the information as spiking patterns in oscillating units [14]–[16], we evaluated the stability of such patterns to changes in initial membrane potentials, connection delays or synaptic weights modelled on histologically verified connections of coupled excitatory and inhibitory neurons, keeping all parameters within their biological limits. The key concept underlying such a study is, thus, the selection of an applied neuronal model to capture the characteristics of many different types of stimulated neurons, their spiking behaviour and their signal dynamics. Many neuron models (for review see [17], [18]) differ in their biological plausibility (high in Hodkin–Huxley-

Manuscript received May 27, 2018; revised October 10, 2018; accepted November 11, 2018. Date of publication November 28, 2018; date of current version March 22, 2019. This work was supported by an Internal Research Grant at the Department of Computing and Control Engineering, University of Chemistry and Technology Prague from the Ministry of Education, Youth and Sports of the Czech Republic. Further support includes the research project MH CZ—DRO (UHHK 00179906) and PROGRES Q40 at the Medical Faculty, Charles University, Czech Republic. *(Corresponding author: Aleš Procházka.)*

P. Cejnar is with the Department of Computing and Control Engineering, University of Chemistry and Technology in Prague, 166 28 Prague, Czech Republic (e-mail: pavel.cejnar@vscht.cz).

O. Vyšata and M. Vališ are with the Department of Neurology, Faculty of Medicine in Hradec Králové, Charles University, 500 03 Hradec Králové, Czech Republic (e-mail: vysatao@gmail.com; valismar@seznam.cz).

A. Procházka is with the Department of Computing and Control Engineering, University of Chemistry and Technology in Prague, 166 28 Prague, Czech Republic, and also with the Czech Institute of Informatics, Robotics and Cybernetics, Czech Technical University in Prague, 160 00 Prague, Czech Republic (e-mail: a.prochazka@ieee.org).

This paper has supplementary downloadable material available at http://ieeexplore.ieee.org, provided by authors.

Digital Object Identifier 10.1109/TNSRE.2018.2883618

type models), computational efficiency (high in integrate-and-fire models) and scope of proper simulation of different types of neurons and their behavioural dynamics [17], [19]. We applied the widely accepted Izhikevich model [19]–[21], which can accurately simulate huge scope of observed biological signals of several types of neurons with adequate computer efficiency [8]. This model is able to generate a large range of empirically accurate spiking behaviours, like the Hodgkin-Huxley equations, while being much easier to compute with. The Izhikevich model is originally continuous-time, but numeric discretization transforms it into the map. It exhibits preferential amplification of inputs at particular frequencies, that is, resonant behaviour. Leaky integrated and fire neuron model (LIF) is another spiking neural network (SNN) model (see also [22]). Both models can be compared in terms of speed and accuracy of learning in artificial neural networks. Though LIF model is faster than Izhikevich model but recognition rate of Izhikevich model is more accurate than the LIF model [23]. LIF fails to exhibit all neuron behaviors e.g. phasic spiking, bursting, and rebound responses being not good enough in simulations [24]. Another used model, Hodgkin-Huxley neuron, is able to model biophysically and biologically meaningful properties of the neuron membrane. However, it is not able to faithfully reproduce the behavior of different types of cortical neurons and is computationally demanding. Its simple representation is the BVP model. It cannot exhibit chaotic dynamics or bursting, so it is not suitable for our simulations. The so-called Hindmarsh–Rose model is biologically plausible but it can be problematic to find appropriate functions F(v), G(v) and H(v) chosen to display the generation of bursts of spikes. Other suitable models include more complex and comutationally less efficient Wilson model, Morris–Lecar model, Spike-response model. Izhikevich model is the only model which can produce neural network activities such as inhabitation-induced bursting, mixed mode activity or phasic bursting [24]. The model allows quantitative reproduction of subthreshold, spiking and bursting activity of all known types of cortical and thalamic neurons [8]. It is one of three SNN models (together with Hindmarsh–Rose model and Hodgkin-Huxley model) able to produce chaotic behaviour. We have chosen the Izhikevich model because it is the only one able to produce all known types of cortical spiking activities.

Spiny stellate cells (SS) are an exclusive category of cortical interneurons and are the major component of intracolumnar, lateral, and callosal excitation of pyramidal and non-pyramidal neurons in the neocortex. The axons of SS make contact with the apical dendrites of pyramidal neurons and establish recurrent connections with inhibitory interneurons and other SS. Pyramidal neurons are the most numerous excitatory cell type in mammalian cortical structures. In cortical layer II there is a mix of interconnected small pyramidal cells and some inhibitory neurons, mainly bipolar cells and double bouquet cells. The apical tuft of pyramidal neurons receives excitatory synaptic inputs that have different presynaptic origins. There is a greater potential for recurrent excitation through re-entrant circuits composed of neurons that integrate large numbers of excitatory inputs and are highly interconnected than in circuits composed of sparsely interconnected neurons that sample relatively few inputs. The tested behaviour of neuronal couplings include excitatory pyramidal and spiny stellate interneurons (regular spiking) and inhibitory GABAergic interneurons—basket interneurons (cells with fast spiking patterns [25] and non-basket interneurons (low-threshold spiking cells, [26]).

If we accept the hypothesis of oscillators as the basic information carriers, then we must verify whether such structures, based on histologically verified connections, are able to show the behaviour similar to the one observed in brain with its ability to preserve the information. We would suppose that these structures would maintain information during conditions similar to reduced brain activity, unfavourable outer conditions or even after any outage of the whole electro-biological activity. In this study, we show for selected modelled couplings of existing pyramidal, spiny stellate interneurons and GABAergic interneurons that these couplings are able to preserve oscillation patterns even in such unfavourable conditions while all the parameters used are kept within their biological limits. We confirm, that the initial levels of membrane potentials and synaptic currents does not lead to significantly different oscillation patterns allowing preserving stored information even when the oscillating activity must be recovered. Then we focus on the dependence of the behaviour of different interneuron signal transmission dynamics on signal transmission delays. According to recent studies, neurons are predominantly connected to the other neurons in their surrounding neighbourhood [27], and a fraction of them are also linked to neurons in other cortical areas [28]. In such a network, changes in oscillatory activity spread easily and were observed to be synchronized even in distant areas of the brain when attracted by a single stimulus, even without synchronization in some cases (experiments on a cat and an awake monkey) [29]–[31]. In that case, relatively robust oscillatory activity behaviour against varying lengths of synaptic paths and, in general, the signal delays is required. The axonal conductance delay varies greatly in the mammalian nervous system from less than 100 microseconds in very short axons up to 100 ms in very long non-myelinated central axons [32], [33]. The different interconnection delays are due to temperature and metabolic conditions, lengths of synaptic paths, axon dimensions or material structure. Even when using accurate differential equation models of neuron activity, the different delays of the signal could affect the behaviour of the resulting oscillation patterns, and thus, the relationship must be confirmed. In contrast to the relatively robust behaviour towards some parameters required to preserve information, other parameters that are capable of significantly changing the oscillatory patterns to modify the represented information must also exist. We suppose that these parameters include the synaptic weight and, according to current models, its conductance. If this is the case, the dependence on the synaptic weight should be very sensitive and strong, even when it varies within its possible biological limits. The behaviour observed when altering the synaptic weights of the oscillating neurons should result in significant changes in the frequency, the phase or, at least, the amplitude area of the signal.

In this paper we show that changes in variation of oscillating patterns behaviour are significantly different in response to changes in the initial levels of membrane potentials, interconnection delays and synaptic weights using all model parameters within their biological limits. Especially, the changes in synaptic weights result in significant increase of peak interval variation and significant decrease in their correlation in comparison to other two studied parameters. Finally, we show that the large number of distinct oscillating frequencies are present in even very small neuron couplings showing potentially high capability for different information encoding when oscillating units are used as basic information storage units.

II. Methods

A. Neuron Coupling

Known, histologically verified neural connections (Fig. 1) were interpreted by a set of differential equations based on the Izhikevich phenomenological model [21]. Neuron behavioural dynamics are simulated using two differential equations for each neuron based on [34]:

$$\dot{v}_i(t) = \frac{1}{C_i}(z_i\,(v_i(t) - r_i)\,(v_i(t) - h_i) - u_i + I_i + \sum_j s_{ij}\,w_{ij}\,v_j(t - d_{ij})) \quad (1)$$

$$\dot{u}_i(t) = a_i\,(b_i\,(v_i(t) - r_i) - u_i(t)) \quad (2)$$

where

- t is the formal time (in ms),
- $v_i(t)$ is the membrane potential (in mV),
- C_i is the membrane capacitance (in pF),
- r_i is the resting potential (in mV),
- h_i is the instantaneous threshold potential (in mV),
- $u_i(t)$ is the recovery variable (the difference between all inward and outward voltage-gated currents, in pA),
- I_i is the approximation of dendritic and synaptic current (in pA),
- s_{ij} is $+1$ or -1 for an excitatory or inhibitory synapse, respectively,
- w_{ij} is the synaptic weight, i.e. the conductance of synapse between neurons i and j (in nS),
- v_j is the membrane potential of neuron j (in mV),
- d_{ij} is the delay of synaptic connection (in ms),
- c_i is the potential reset value (in mV),
- e_i is the outward minus inward currents activated during the spike and affecting the afterspike behavior (in pA),

and z_i (in nS), a_i (in ms^{-1}) and b_i (in nS) are predefined constants depending on the neuron type, as explained below.

As soon as the membrane potential reaches the critical level v_{peak}, spike firing is evoked. The individual variables $v_i(t)$ and $u_i(t)$ for the given neuron are reset to values $v_i(t) \leftarrow c_i$ and $u_i(t) \leftarrow u_i(t) + e_i$.

The parameters of the individual neuronal subtypes are listed in Table I. For the non-basket neurons, the value of the recovery variable is maintained below 670 pA; i.e., if a higher value of the recovery variable $u_i(t)$ is calculated, this value is set to $u_i(t) = 670$ pA.

TABLE I

PARAMETERS USED FOR SPECIFIC NEURONAL SUBTYPES (NS) BASED ON [8] AND [21]. (i) SUBTYPES OF CORTICAL EXCITATORY NEURONS: *p3–p6* — PYRAMIDAL NEURONS IN THE CORRESPONDING L3–L6 AREA OF THE BRAIN, *ss4* — SPINY STELLATE NEURONS IN AREA L4 OF THE BRAIN AND (ii) SUBTYPES OF GABAERGIC (INHIBITORY) NEURONS: *b* — BASKET INTERNEURON, *nb* — NON-BASKET INTERNEURON

NS	C	z	r	h	I	a	b	v_{peak}	c	e
	pF	nS	mV	mV	pA	ms^{-1}	nS	mV	mV	pA
p3	100	3	−60	−50	500	0.01	5	50	−60	400
p4	100	3	−60	−50	500	0.01	5	50	−60	400
p5	100	3	−60	−50	500	0.01	5	50	−60	400
p6	100	3	−60	−50	500	0.01	5	50	−60	400
ss4	100	3	−60	−50	250	0.01	5	50	−60	400
b	20	1	−55	−40	250	0.15	8	25	−55	200
nb	100	1	−56	−42	300	0.03	8	40	−50	20

B. Bio-Physical Properties of the Modelled Neuron

To produce satisfactory results, most of the common models of biological neural networks require the presence of noise. This biological noise should result from synaptic noise [21], [35]. The oscillatory activity of modelled oscillators is generally dependent on the input signal and can result from synaptic noise or the activity of surrounding neurons [21]. To obtain insight into the intrinsic activity of oscillators and the behaviour of surrounding neurons, we used a constant zero-input signal and focused on the intrinsic oscillatory behaviour of selected neural connections.

The conductance of individual synapses ranging from 0.6 to 5.0 nS was assessed to characterize the parameters of each neuron [36]. With a proper coupling of two sequential compartments, we would expect the potential or current change to range from 0.1× to 10×. To avoid speculating on extreme coupling, we limited our focus to connection weights in the range of 0.5–6.5 nS. In this range, the weight of each selected connection was gradually modified, and the intervals between the individual peaks that occurred in the membrane potential signal of each chosen neuron were measured.

To obtain relevant results, the total current in the neurons was estimated and correlated with known spiking and bursting activity for the modelling of individual neurons. The estimated currents are also listed in Table I.

The experimental studies of the biophysical properties of neuron cells show synaptic delays in the range of 0.1 ms to 44 ms [32], [33]; thus, we decide to limit the experiments to delays in the range of 0 to 20 ms with exception of one selected coupling, where the range was broadened (0 to 1000 ms) to confirm the similar behaviour.

C. Differential Equation Solution and Its Confirmation

Euler's method to find a numerical solution of the oscillatory activity for a selected set of couplings was insufficient for the required calculations. Therefore, the differential equations were numerically solved using the Runge–Kutta (RK4) method with root interpolation implemented in Java 1.8 and an elementary step of 0.01 ms [37], which was sufficiently accurate, even with 10^6–10^8 iteration steps in the investigated interval. The numerical stability of the results was confirmed

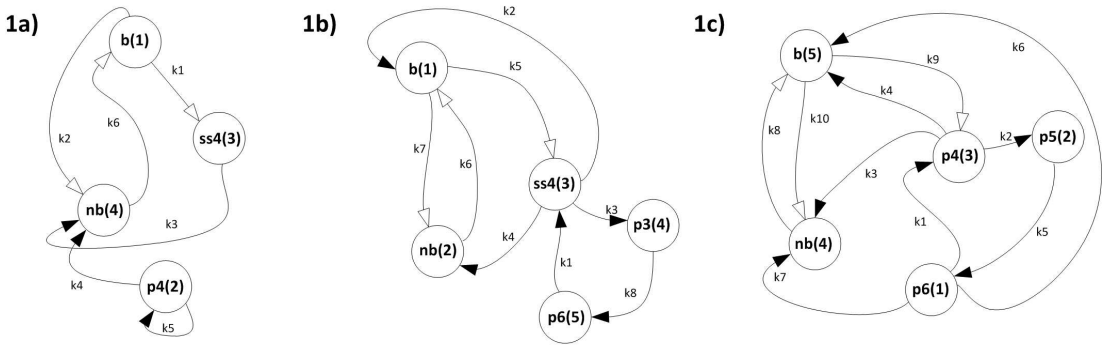

Fig. 1. Tested schemes 1a, 1b, and 1c of histologically verified neuron couplings with the type and the number (in the parentheses) of each neuron (see also [8] and [21]) Connections from excitatory neurons are depicted with black arrow heads, connections from inhibitory neurons are depicted with white arrow heads. The parameters used to simulate their behavioural patterns are listed in Table I.

via comparison against solutions with smaller iteration steps and those obtained by the Livermore Solver for Ordinary Differential Equations (LSODAR) method with the root-finding capability [38] implemented in the Scilab 5.5 environment.

D. Verification of Oscillator Behavioural Diversity

For given coupling C let T_C be the set of all examined instantiations, where for each $\tau_i \in T_C$

$$\tau_i = \langle d_1 \cdots d_{|E_C|}, w_1 \cdots w_{|E_C|}, v_1 \cdots v_{|N_C|}, u_1 \cdots u_{|N_C|} \rangle$$

N_C	is the set of neurons in given coupling C,
E_C	is the set of neuron interconnections in given coupling C,
$d_1, \ldots, d_{\lvert E_C \rvert}$	are delays of given interconnections, $d_i \in \langle 0, 20 \rangle$ ms,
$w_1, \ldots, w_{\lvert E_C \rvert}$	are synaptic weights of given interconnections, $w_i \in \langle 0.5, 6.5 \rangle$ nS,
$v_1, \ldots, v_{\lvert N_C \rvert}$	are initial values of the membrane potential, $v_i \in \langle c_i, v_{peak} \rangle$ according to the type of each neuron, see Fig. 1 and Table I,
$u_1, \ldots, u_{\lvert N_C \rvert}$	are initial differences between inward and outward currents, $u_i \in \langle -e_i, e_i \rangle$ according to the type of each neuron, see Fig. 1 and Table I.

For given coupling C let $S_{d20,C}$, $S_{d1000,C}$, $S_{w,C}$, $S_{vu,C}$ be a set of specific delays up to 20 ms or specific delays up to 1000 ms or synaptic weights or initial membrane potentials and recovery variables respectively, i.e.

$$\begin{aligned}
s_j &= \langle d_1 \cdots d_{|E_C|} \rangle, \quad s_j \in S_{d20,C}, \ d_i \in \langle 0, 20 \rangle \text{ ms} \\
s_j &= \langle d_1 \cdots d_{|E_C|} \rangle, \quad s_j \in S_{d1000,C}, \ d_i \in \langle 0, 1000 \rangle \text{ ms} \\
s_j &= \langle w_1 \cdots w_{|E_C|} \rangle, \quad s_j \in S_{w,C}, \ w_i \in \langle 0.5, 6.5 \rangle \text{ nS} \\
s_j &= \langle v_1 \cdots v_{|N_C|}, u_1 \cdots u_{|N_C|} \rangle, \\
&\qquad s_j \in S_{vu,C}, \ v_i \in \langle c_i, p_i \rangle, \ u_i \in \langle -e_i, e_i \rangle
\end{aligned}$$

according to the type of each neuron, see Fig. 1 and Table I. Based on a given instantiation $\tau_i \in T_C$ and set of specific questioned parameters, for example $s_j \in S_{d20,C}$, we denote $s_j \to \tau_i$ as the τ_i instantiation of the model, where all the values of s_j replaced the appropriate values of τ_i.

To verify the diversity in the oscillator behaviour for studied couplings and different instantiations and parameter sets we selected one connection in the coupling and iteratively examined the results while gradually changing the weight of the connection from 0.5 to 6.5 nS using steps of 0.1 nS. We denote then $\tau_i \downarrow w_k$ or $s_j \to \tau_i \downarrow w_k$ as the τ_i or $s_j \to \tau_i$ instantiation of the model, where the weight of connection k was replaced by the value w_k. For each experiment, the connection was selected from the core of the oscillator in which two neurons are connected to each other by inhibitory synapses with a third neuron interconnecting them by one inhibitory and one excitatory synapse.

For each coupling and its set of 50 or 100 random instantiations $\tau_i \in T_C$ and each investigated parameter X using set of 50 or 100 random parameter sets $s_j \in S_{X,C}$ we determined the peak intervals for each $s_j \to \tau_i$ by solving differential equations in the time interval of 0–20,000 ms. Initial segments with aperiodic behaviour (0–9,000 ms) were eliminated until the neuronal potentials stabilized. To characterize the oscillatory activity behaviour, we computed the descriptive statistic values focusing on coefficients of variation and correlation coefficients. For current instantiation of the model $s_j \to \tau_i \downarrow w_k$, evaluating selected parameter set $S_{X,C}$, let $l_{n(k)_a, w_k}(s_j \to \tau_i \downarrow w_k)$ be the mean value of the peak intervals in the evaluated interval of 9,000 – 20,000 ms at neuron $n(k)_a$. For given neuron $n(k)_a$ and the fixed weight w_k of connection k, if $l_{n(k)_a, w_k}(s_j \to \tau_i \downarrow w_k)$ is seen as a function of s_i, then we compute $L_{n(k)_a, w_k, S_{X,C}}(\tau_i \downarrow w_k)$, an unbiased estimate of coefficient of variation [39] over all $s_i \in S_{X,C}$:

$$\begin{aligned}
&L_{n(k)_a, w_k, S_{X,C}}(\tau_i \downarrow w_k) \\
&\qquad = \left(1 + \frac{1}{4\left|S_{X,C}\right|}\right) \frac{\underset{s_i \in S_{X,C}}{\text{sd}} \left(l_{n(k)_a, w_k}(s_j \to \tau_i \downarrow w_k)\right)}{\underset{s_i \in S_{X,C}}{\text{mean}} \left(l_{n(k)_a, w_k}(s_j \to \tau_i \downarrow w_k)\right)}
\end{aligned}$$

Then we computed the mean values of these estimates of coefficients of variation over each examined weight $w_k \in W = \langle 0.5, 6.5 \rangle$ nS of selected connection k, i.e.

$\underset{w_k \in W}{\text{mean}}(L_{n(k)_a,w_k,S_{X,C}}(\tau_i \downarrow w_k))$ and for both neurons $n(k)_1$, $n(k)_2$ determined the minimum and maximum values. Here, we report the minimum and maximum values of these over the whole set of T_C, i.e.

$$\begin{aligned}
\underset{T_C,k,S_{X,C}}{\text{HiMaxV}} &= \max_{\tau_i \in T_C} \max_{n(k)_a} \underset{w_k \in W}{\text{mean}}(L_{n(k)_a,w_k,S_{X,C}}(\tau_i \downarrow w_k)) \\
\underset{T_C,k,S_{X,C}}{\text{LoMaxV}} &= \min_{\tau_i \in T_C} \max_{n(k)_a} \underset{w_k \in W}{\text{mean}}(L_{n(k)_a,w_k,S_{X,C}}(\tau_i \downarrow w_k)) \\
\underset{T_C,k,S_{X,C}}{\text{LoMinV}} &= \min_{\tau_i \in T_C} \min_{n(k)_a} \underset{w_k \in W}{\text{mean}}(L_{n(k)_a,w_k,S_{X,C}}(\tau_i \downarrow w_k))
\end{aligned}$$

Similarly, the same method was applied using Pearson correlation coefficients. First the detected neuron oscillation patterns were characterized by weighted peak intervals histogram. For given instantiation of the model $s_j \rightarrow \tau_i \downarrow w_k$ evaluating selected parameter set $S_{X,C}$ at neuron $n(k)_a$ with the fixed weight w_k for connection k, the log_2 values of peak intervals from the evaluated interval of 9,000 – 20,000 ms were binned to histogram over the range of $\langle 0, 14\rangle$ fractionated to $(1 + 14 \times 32)$, $(1 + 14 \times 64)$, respective $(1 + 14 \times 128)$ bins covering all possible detected peak intervals starting from 1 ms. The peak intervals bellow 1 ms were added to a separated (the first) bin. Each binned peak interval value was then weighted by its size and normalized by total length of the interval (11,000 ms). The weighted peak intervals histogram can then be viewed as the fractionation of all 11,000 ms of the interval to bins according to peak interval they occur in, using bins in the log_2 scale. Such a histogram with $(1 + 14 \times Z)$ bins is also annotated as $H_{Z,n(k)_a,w_k}(s_j \rightarrow \tau_i \downarrow w_k)$. For given instantiation of the model $\tau_i \downarrow w_k$, selected set of evaluated parameters $S_{X,C}$, selected neuron $n(k)_a$ and the selected fixed weight $w_k \in W = \langle 0.5, 6.5\rangle$ nS of connection k, we computed the mean of correlation coefficients:

$$\begin{aligned}
&C_{Z,n(k)_a,w_k,S_{X,C}}(\tau_i \downarrow w_k) \\
&\quad = \underset{s_x \neq s_y \in S_{X,C}}{\text{mean}} \text{cor}(H_{Z,n(k)_a,w_k}(s_x \rightarrow \tau_i \downarrow w_k), \\
&\qquad\qquad H_{Z,n(k)_a,w_k}(s_y \rightarrow \tau_i \downarrow w_k)) \qquad (3)
\end{aligned}$$

This coefficient is seen as descriptive only, no Fisher Z-transformation was used due to non-rare occurence of 1.0 correlation values. The similar minimum and maximum values are then reported:

$$\begin{aligned}
\underset{Z,T_C,k,S_{X,C}}{\text{HiMaxC}} &= \max_{\tau_i \in T_C} \max_{n(k)_a} \underset{w_k \in W}{\text{mean}}(C_{Z,n(k)_a,w_k,S_{X,C}}(\tau_i \downarrow w_k)) \\
\underset{Z,T_C,k,S_{X,C}}{\text{LoMaxC}} &= \min_{\tau_i \in T_C} \max_{n(k)_a} \underset{w_k \in W}{\text{mean}}(C_{Z,n(k)_a,w_k,S_{X,C}}(\tau_i \downarrow w_k)) \\
\underset{Z,T_C,k,S_{X,C}}{\text{LoMinC}} &= \min_{\tau_i \in T_C} \min_{n(k)_a} \underset{w_k \in W}{\text{mean}}(C_{Z,n(k)_a,w_k,S_{X,C}}(\tau_i \downarrow w_k))
\end{aligned}$$

This allowed us to better present the diversity behaviour using different $S_{X,C}$ classes.

To determine the effect of scaling, first the results for $|T_C| = 50$ and $|S_{X,C}| = 50$ for each investigated parameter were computed. Then the computations were scaled to $|T_C| = 100$ and $|S_{X,C}| = 50$ and finally the experiment was run for $|T_C| = 100$ and $|S_{X,C}| = 100$. The computations were performed on a PC with two quad-core Intel Xeon E5540 processors and 16 GB of RAM and took approximately 10 days for each coupling and investigated parameter.

E. Confirmation of Oscillator Behavioural Diversity

The Welch two-sided t-test was applied to $L_{n(k)_a,w_k,S_{X,C}}(\tau_i \downarrow w_k)$ and $C_{Z,n(k)_a,w_k,S_{X,C}}(\tau_i \downarrow w_k)$ for each pair of tested parameter sets $S_{X,C}$ for given coupling C, given template set T_C, and all weights $w_k \in W = \langle 0.5, 6.5\rangle$ nS for selected connection k using 0.1 nS weight step. Welch approximation to the degrees of freedom was used for estimation of variance (unequal variances). The mean value estimates are also reported:

$$\begin{aligned}
\overline{L_{T_C,k,S_{X,C}}} &= \underset{\tau_i \in T_C, w_k \in W}{\text{mean}}(L_{n(k)_a,w_k,S_{X,C}}(\tau_i \downarrow w_k)) \\
\overline{C_{Z,T_C,k,S_{X,C}}} &= \underset{\tau_i \in T_C, w_k \in W}{\text{mean}}(C_{Z,n(k)_a,w_k,S_{X,C}}(\tau_i \downarrow w_k))
\end{aligned}$$

F. Detection of Oscillation Patterns Capacity

For given template $\tau_i \in T_C$, maximum allowed histogram correlation γ, Z bins for each order of magnitude in weighted histograms, given neuron $n(k)_a$ from connection k and evaluated parameter set $S_{X,C}$, the $F_{\gamma,Z,n(k)_a,k,S_{X,C}}(\tau_i \downarrow w_k)$ estimates the number of distinct oscillation patterns on given neuron $n(k)_a$, when the weight $w_k \in \langle 0.5, 6.5\rangle$ nS for connection k is gradually changing using 0.1 nS weight step:

$$\begin{aligned}
&F_{\delta,Z,n(k)_a,k,S_{X,C}}(\tau_i) \\
&\quad = \max_{s_j \in S_{X,C}} \max \text{card}(\omega_x : x = 1..N, \omega_x < \omega_{x+1}, \\
&\qquad \text{cor}(H_{Z,n(k)_a,w_k=\omega_x}(s_j \rightarrow \tau_i \downarrow w_k), \\
&\qquad H_{Z,n(k)_a,w_k=\omega_{x+1}}(s_j \rightarrow \tau_i \downarrow w_k)) \leq \gamma)
\end{aligned}$$

Maximum and minimum values over T_C set and both neurons $n(k)_a$ of gradually changing connection k for selected coupling and evaluated parameter set $S_{X,C}$ are then reported:

$$\begin{aligned}
\underset{\gamma,Z,T_C,k,S_{X,C}}{\text{HiMaxF}} &= \max_{\tau_i \in T_C} \max_{n(k)_a} F_{\gamma,Z,n(k)_a,k,S_{X,C}}(\tau_i) \\
\underset{\gamma,Z,T_C,k,S_{X,C}}{\text{LoMaxF}} &= \min_{\tau_i \in T_C} \max_{n(k)_a} F_{\gamma,Z,n(k)_a,k,S_{X,C}}(\tau_i) \\
\underset{\gamma,Z,T_C,k,S_{X,C}}{\text{LoMinF}} &= \min_{\tau_i \in T_C} \min_{n(k)_a} F_{\gamma,Z,n(k)_a,k,S_{X,C}}(\tau_i)
\end{aligned}$$

III. Results

Using the Izhikevich phenomenological model of known neuron subtypes, here, we characterize the oscillatory behaviour of histologically verified excitatory neurons that are coupled in circuits through inhibitory interneurons (basket and non-basket inhibitory cells). For a selected set of neuron couplings (Fig. 1), we studied the dependence of the acquired oscillatory activity (detected peak intervals) on different parameters.

First a large-scale simulation of different initial electrophysical conditions was run and the dependence on different initial values of membrane potential and recovery variables was studied. For each tested coupling and each of its 50 or 100 random instantiations we evaluated 50 and then 100 different random initial membrane potentials and values of their recovery variables. For detected coefficients of variation and correlation coefficients for tested parameter sets $S_{vu,C}$ appropriate for each coupling, see Table II, Table III and Table IV. As a visual example, for one coupling

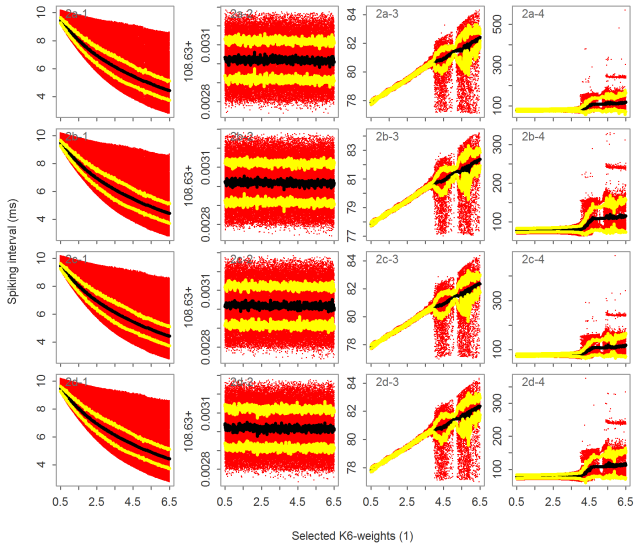

Fig. 2. The dependence of oscillatory activity on different initial values of membrane potential and recovery variables of given coupling (Fig. 1(1a)) for (2a) neurons n_1–n_4 with all membrane potentials and recovery variables initially set to zero, (2b) neurons n_1–n_4 with initial membrane potentials set to $v_{1,\ldots,4} = [24.0, 49.0, 49.0, 39.0]$ and recovery variables $u_{1,\ldots,4} = [0.0, 0.0, 0.0, 0.0]$, (2c) neurons n_1–n_4 with an initial setting of the membrane potential at $v_{1,\ldots,4} = [-55.0, -60.0, -60.0, -50.0]$ and recovery variables at $u_{1,\ldots,4} = [0.0, 0.0, 0.0, 0.0]$, and (2d) neurons n_1–n_4 with initial settings of the membrane potential at $v_{1,\ldots,4} = [24.0, -60.0, 49.0, -50.0]$ and recovery variables at $u_{1,\ldots,4} = [200.0, 400.0, -400.0, 20.0]$. The mean value (black) ± one sample standard deviation (yellow) interval is also indicated.

(Fig. 1(1a)), the time intervals between subsequent peaks in individual neurons n_1–n_5 for different initial settings are also presented (Fig. 2) as the selected synaptic weight of selected conection (here k_6) was changing. In the given coupling, the weights of individual connections $w_{1,\ldots,6} = [5.36, 4.31, 4.31, 2.11, 2.72, 1.56]$ and the delays of individual connections $d_{1,\ldots,6} = [19.22, 7.4, 2.28, 2.48, 16.53, 10.88]$ were considered. In Fig. 2 the mean value (black) ± one sample standard deviation (yellow) is also marked.

Next, the dependence of oscillatory activity on different connection delays was evaluated. The computed statistical coefficients for 50 and then 100 random instantiations evaluated with 50 and then 100 different random connection delays ($S_{d20,C}$ parameter set) are presented in Table II, Table III and Table IV according to selected coupling. The increased variation of peak intervals and decreased correlation of peak interval histograms show the increased sensitivity in comparison to previously tested dependence on different initial values of membrane potential and recovery variables. To confirm the behaviour of the diversity in this parameter, we ran another simulation with even more prolonged connection delays. For the selected coupling (Fig. 1(1a)), we monitored the level of diversity at connection delays as long as 1000 ms (S_{d1000,C_1} parameter set), which could exceed the biological limits, however, only a small additional change in diversity was observed. The example of changes in oscillatory activity induced by different interneuron connection delays for a selected coupling (Fig. 1(1a)) is presented in Fig. 3. The time intervals between subsequent peaks in individual neurons n_1–

TABLE II
THE DIVERSITY IN THE BEHAVIOUR OF THE SELECTED COUPLING (FIG. 1(1a)) AND ITS RESPONSE TO CHANGES IN VARIOUS PARAMETERS: RANDOMLY INITIALIZED MEMBRANE POTENTIALS AND RECOVERY VARIABLE VALUES, INTERCONNECTION DELAYS, AND CONNECTION WEIGHTS

$\|T_C\|$=50, $\|S_{X,C}\|$=50				
	$S_{vu,C}$	$S_{d20,C}$	$S_{d1000,C}$	$S_{w,C}$
HiMaxV$_{T_C,k_6,S_{X,C}}$	0.09759	0.16672	0.14879	0.93200
LoMaxV$_{T_C,k_6,S_{X,C}}$	0.00007	0.00528	0.00537	0.84115
LoMinV$_{T_C,k_6,S_{X,C}}$	0.00002	0.00080	0.00124	0.57407
HiMaxC$_{128,T_C,k_6,S_{X,C}}$	0.99942	0.99883	0.99831	0.30894
LoMaxC$_{128,T_C,k_6,S_{X,C}}$	0.95369	0.88187	0.92800	0.30492
LoMinC$_{128,T_C,k_6,S_{X,C}}$	0.70541	0.50898	0.40567	0.06300
$\|T_C\|$=100, $\|S_{X,C}\|$=50				
	$S_{vu,C}$	$S_{d20,C}$	$S_{d1000,C}$	$S_{w,C}$
HiMaxV$_{T_C,k_6,S_{X,C}}$	0.09759	0.16672	0.14879	0.94979
LoMaxV$_{T_C,k_6,S_{X,C}}$	0.00005	0.00528	0.00401	0.84115
LoMinV$_{T_C,k_6,S_{X,C}}$	0.00002	0.00080	0.00109	0.57407
HiMaxC$_{128,T_C,k_6,S_{X,C}}$	0.99943	0.99883	0.99832	0.33436
LoMaxC$_{128,T_C,k_6,S_{X,C}}$	0.95374	0.88185	0.92949	0.32979
LoMinC$_{128,T_C,k_6,S_{X,C}}$	0.70547	0.51820	0.40377	0.06989
$\|T_C\|$=100, $\|S_{X,C}\|$=100				
	$S_{vu,C}$	$S_{d20,C}$	$S_{d1000,C}$	$S_{w,C}$
HiMaxV$_{T_C,k_6,S_{X,C}}$	0.10371	0.15677	0.15394	0.84991
LoMaxV$_{T_C,k_6,S_{X,C}}$	0.00005	0.00532	0.00391	0.74193
LoMinV$_{T_C,k_6,S_{X,C}}$	0.00002	0.00072	0.00107	0.62115
HiMaxC$_{128,T_C,k_6,S_{X,C}}$	0.99943	0.99883	0.99832	0.34722
LoMaxC$_{128,T_C,k_6,S_{X,C}}$	0.95374	0.81997	0.91116	0.32979
LoMinC$_{128,T_C,k_6,S_{X,C}}$	0.65612	0.35856	0.13404	0.06738

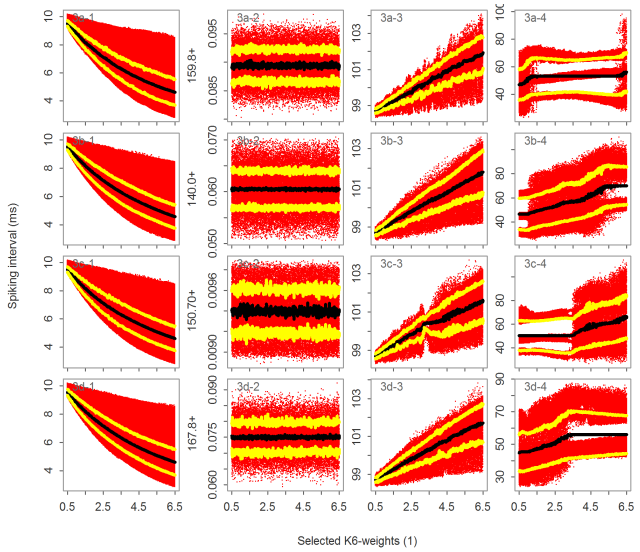

Fig. 3. The dependence of oscillatory activity on different delay levels in individual synapses of selected coupling (Fig. 1(1a)) for (3a) interneuron connection delay of neurons n_1–n_4 at $d_{1,\ldots,6} = [571.81, 27.31, 773.97, 481.86, 542.78, 34.46]$, (3b) interneuron connection delay of neurons n_1–n_4 at $d_{1,\ldots,6} = [455.8, 252.04, 632.29, 840.31, 277.09, 416.25]$, (3c) interneuron connection delay for neurons n_1–n_4 at $d_{1,\ldots,6} = [590.25, 666.13, 121.91, 283.65, 18.82, 496.77]$, and (3d) interneuron connection delay for neurons n_1–n_4 at $d_{1,\ldots,6} = [333.13, 86.36, 958.17, 806.81, 272.52, 227.05]$. The mean value (black) ± one sample standard deviation (yellow) is indicated.

n_4 for different connection delays are presented while the synaptic weight of selected connection (here k_6) was changing. In the selected coupling, the weights of individual connec-

TABLE III
THE DIVERSITY IN THE BEHAVIOUR OF THE SELECTED COUPLING (FIG. 1(1b)) AND ITS RESPONSE TO CHANGES IN VARIOUS PARAMETERS: RANDOMLY INITIALIZED MEMBRANE POTENTIALS AND RECOVERY VARIABLE VALUES, INTERCONNECTION DELAYS, AND CONNECTION WEIGHTS

$\lvert T_C\rvert$=50, $\lvert S_{X,C}\rvert$=50			
	$S_{vu,C}$	$S_{d20,C}$	$S_{w,C}$
HiMaxV$_{T_C,k_6,S_{X,C}}$	0.005921	0.095509	0.931525
LoMaxV$_{T_C,k_6,S_{X,C}}$	0.000008	0.002670	0.826745
LoMinV$_{T_C,k_6,S_{X,C}}$	0.000008	0.001083	0.588584
HiMaxC$_{128,T_C,k_6,S_{X,C}}$	0.999436	0.890544	0.087794
LoMaxC$_{128,T_C,k_6,S_{X,C}}$	0.874197	0.236162	0.075564
LoMinC$_{128,T_C,k_6,S_{X,C}}$	0.002107	−0.00069	0.040358
$\lvert T_C\rvert$=100, $\lvert S_{X,C}\rvert$=50			
	$S_{vu,C}$	$S_{d20,C}$	$S_{w,C}$
HiMaxV$_{T_C,k_6,S_{X,C}}$	0.005921	0.095509	0.949795
LoMaxV$_{T_C,k_6,S_{X,C}}$	0.000008	0.002351	0.826492
LoMinV$_{T_C,k_6,S_{X,C}}$	0.000008	0.000832	0.576190
HiMaxC$_{128,T_C,k_6,S_{X,C}}$	0.999431	0.891707	0.087594
LoMaxC$_{128,T_C,k_6,S_{X,C}}$	0.878124	0.240672	0.076064
LoMinC$_{128,T_C,k_6,S_{X,C}}$	0.001495	0.015842	0.046868
$\lvert T_C\rvert$=100, $\lvert S_{X,C}\rvert$=100			
	$S_{vu,C}$	$S_{d20,C}$	$S_{w,C}$
HiMaxV$_{T_C,k_6,S_{X,C}}$	0.005960	0.094954	0.880070
LoMaxV$_{T_C,k_6,S_{X,C}}$	0.000008	0.002399	0.758187
LoMinV$_{T_C,k_6,S_{X,C}}$	0.000008	0.000858	0.627207
HiMaxC$_{128,T_C,k_6,S_{X,C}}$	0.999431	0.891707	0.088907
LoMaxC$_{128,T_C,k_6,S_{X,C}}$	0.756507	0.213391	0.076064
LoMinC$_{128,T_C,k_6,S_{X,C}}$	0.001495	0.015842	0.046818

TABLE IV
THE DIVERSITY IN THE BEHAVIOUR OF SELECTED COUPLING (FIG. 1(1c)) AND ITS RESPONSE TO CHANGES IN VARIOUS PARAMETERS: RANDOMLY INITIALIZED MEMBRANE POTENTIALS AND RECOVERY VARIABLE VALUES, INTERCONNECTION DELAYS, AND CONNECTION WEIGHTS

$\lvert T_C\rvert$=50, $\lvert S_{X,C}\rvert$=50			
	$S_{vu,C}$	$S_{d20,C}$	$S_{w,C}$
HiMaxV$_{T_C,k_{10},S_{X,C}}$	0.002030	0.017426	0.353601
LoMaxV$_{T_C,k_{10},S_{X,C}}$	0.000097	0.000532	0.347084
LoMinV$_{T_C,k_{10},S_{X,C}}$	0.000081	0.000167	0.322075
HiMaxC$_{128,T_C,k_{10},S_{X,C}}$	0.992350	0.804485	0.052245
LoMaxC$_{128,T_C,k_{10},S_{X,C}}$	0.722670	0.107465	0.044803
LoMinC$_{128,T_C,k_{10},S_{X,C}}$	0.291564	0.035869	0.013190
$\lvert T_C\rvert$=100, $\lvert S_{X,C}\rvert$=50			
	$S_{vu,C}$	$S_{d20,C}$	$S_{w,C}$
HiMaxV$_{T_C,k_{10},S_{X,C}}$	0.003174	0.017426	0.353601
LoMaxV$_{T_C,k_{10},S_{X,C}}$	0.000097	0.000532	0.344530
LoMinV$_{T_C,k_{10},S_{X,C}}$	0.000064	0.000167	0.322075
HiMaxC$_{128,T_C,k_{10},S_{X,C}}$	0.992356	0.806635	0.053498
LoMaxC$_{128,T_C,k_{10},S_{X,C}}$	0.722286	0.100988	0.046980
LoMinC$_{128,T_C,k_{10},S_{X,C}}$	0.337778	0.035266	0.014689
$\lvert T_C\rvert$=100, $\lvert S_{X,C}\rvert$=100			
	$S_{vu,C}$	$S_{d20,C}$	$S_{w,C}$
HiMaxV$_{T_C,k_{10},S_{X,C}}$	0.003173	0.015977	0.409629
LoMaxV$_{T_C,k_{10},S_{X,C}}$	0.000099	0.000521	0.402831
LoMinV$_{T_C,k_{10},S_{X,C}}$	0.000065	0.000191	0.363295
HiMaxC$_{128,T_C,k_{10},S_{X,C}}$	0.999423	0.825275	0.054085
LoMaxC$_{128,T_C,k_{10},S_{X,C}}$	0.649125	0.100988	0.046980
LoMinC$_{128,T_C,k_{10},S_{X,C}}$	0.162575	0.035266	0.014689

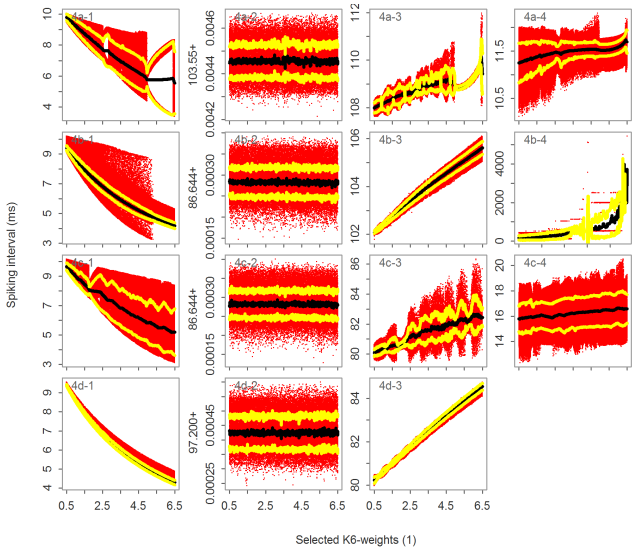

Fig. 4. The dependence of oscillatory activity on different individual synapse weights of given coupling (Fig. 1(1a)) for (4a) neurons n_1–n_4 with weights set at $w_{1,\ldots,6}$ = [2.0, 5.0, 0.5, 0.5, 2.5, 2.0], (4b) neurons n_1–n_4 with weights set at $w_{1,\ldots,6}$ = [2.5, 6.5, 2.5, 6.5, 1.0, 2.5], (4c) neurons n_1–n_4 with weights set at $w_{1,\ldots,6}$ = [5.0, 5.0, 0.5, 2.5, 1.0, 6.5], and (4d) neurons n_1–n_4 with weights set at $w_{1,\ldots,6}$ = [5.0, 1.0, 2.0, 2.5, 2.0, 6.5].

TABLE V
WELCH t-TEST MEAN ESTIMATES FOR TESTING THE SIGNIFICANCE OF DIFFERENCE OF MEANS FOR CORRELATION COEFFICIENTS AND COEFFICIENTS OF VARIATION FOR ALL THREE TESTED COUPLINGS. t-TEST p-VALUES FOR SIGNIFICANCE OF MEANS BETWEEN EACH TWO TESTED PARAMETERS SETS FOR EACH COUPLING AND TESTED COEFFICIENTS WERE ALL BELLOW 1×10^{-34}. THE MEANS OF COEFFICIENTS WERE COMPUTED USING DETECTED COEFFICIENTS FOR $\lvert T_C\rvert = 100$, $\lvert S_{X,C}\rvert = 100$

Coupling 1 (Fig. 1(1a))			
	$S_{vu,C}$	$S_{d20,C}$	$S_{w,C}$
$\overline{L_{T_C,k_6,S_{X,C}}}$	0.00537624	0.02919480	0.73044923
$\overline{C_{128,T_C,k_6,S_{X,C}}}$	0.93479463	0.86554442	0.20271878
Coupling 2 (Fig. 1(1b))			
$\overline{L_{T_C,k_6,S_{X,C}}}$	0.00086194	0.00984183	0.74552863
$\overline{C_{128,T_C,k_6,S_{X,C}}}$	0.92627692	0.58090027	0.06704873
Coupling 3 (Fig. 1(1c))			
$\overline{L_{T_C,k_{10},S_{X,C}}}$	0.00040243	0.00360594	0.38554005
$\overline{C_{128,T_C,k_{10},S_{X,C}}}$	0.85705153	0.40378584	0.03462147

tions $w_{1,\ldots,6}$ = [2.81, 4.91, 0.82, 5.15, 4.63, 5.59], the initial membrane potentials $v_{1,\ldots,4}$ = [−17.23, 27.61, −57.93, 39.63] and the initial setting of recovery variables $u_{1,\ldots,4}$ = [−119.75, 193.36, −0.64, 9.5] were considered.

Finally, the dependence of oscillatory activity on synaptic weights using appropriate $S_{w,C}$ parameter set for each tested

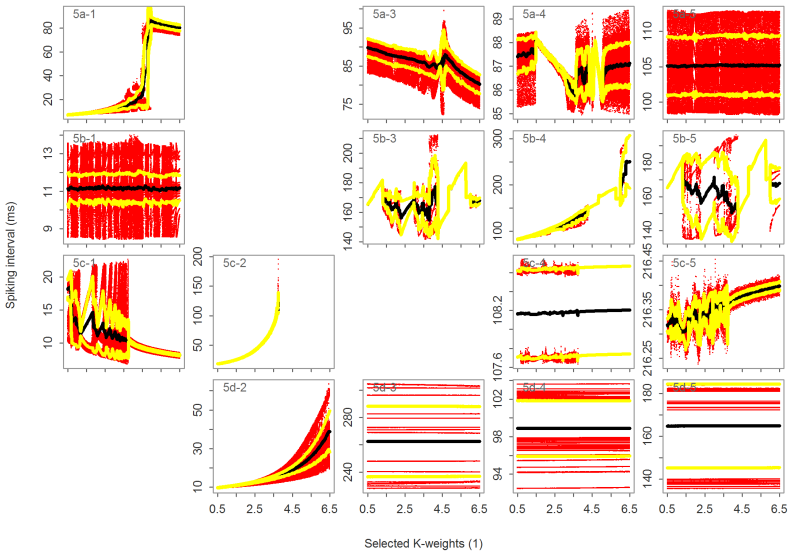

Fig. 5. The dependence of oscillatory activity on different weights in individual synapses of selected coupling (Fig. 1(1b)). The neurons where no oscillatory activity occurred at given setting are omitted. (5a) neurons n_1, n_3–n_5 with weights set at $w_{1,\ldots,8} = [2.0, 1.0, 1.0, 6.5, 6.5, 2.5, 1.0, 2.5]$ changing the w_2 weight, (5b) neurons n_1, n_3–n_5 with weights set at $w_{1,\ldots,8} = [5.0, 2.5, 6.5, 5.0, 5.0, 2.5, 1.0, 5.0]$ while the w_3 weight was changing, (5c) neurons n_1, n_2, n_4, n_5 with weights set at $w_{1,\ldots,8} = [6.5, 5.0, 2.5, 1.0, 1.0, 6.5, 1.0, 6.5]$ while the w_4 weight was changing and (5d) neurons n_2–n_5 with weights set at $w_{1,\ldots,8} = [2.5, 5.0, 2.0, 1.0, 0.5, 0.5, 5.0, 5.0]$ while the w_4 weight was changing.

coupling was evaluated. The example of dependence of the temporal interval between peaks on different synaptic weight sets is shown in Fig. 4. For this figure the results for coupling (Fig. 1(1a)) are present while the synaptic weight of connection k_6 was changing. In the given coupling, the delay of individual connections at $d_{1,\ldots,6} = [4.0, 3.0, 9.0, 18.0, 2.5, 4.5]$ and the initial setting of all membrane potentials and recovery variables to zero were considered. Computed statistical coefficients for 50 and then 100 random instantiations evaluated with 50 and then 100 different random synaptic weights are presented in Table II, Table III and Table IV. The significant increase in variation and significant decrease in correlation of weighted peak interval histograms in comparison to previously tested parameters generally indicates strong dependence of oscillation patterns on the synaptic weight of selected intra-coupling connections. The same general decrease trend for correlation coefficients of weighed peak interval histograms for tested parameter sets $S_{vu,C}$, $S_{d20,C}$, $S_{w,C}$ for different number of bins ($1 + 14 \times 64$ and $1 + 14 \times 32$) is also visible (see Supplement Table S-I, S-II).

The sensitivity described by detected changes in coefficients of variation and in correlation coefficients of weighed peak interval histograms was tested while changing synaptic weight of one randomly selected connection from the core of the oscillator and thus allowing the confirmation of the trends for coefficients of variation and correlation coefficients over the couplings. For each tested parameter set and coupling only a small amount of detected $C_{Z,n(k)_a,w_k,S_{X,C}}(\tau_i \downarrow w_k)$ coefficients were negative and, in that case, their absolute values were close to zero. The resulted mean values (see also Table V) are then affected by these negative coefficients only in a limited way. All t-test p-values for testing significance in difference of means (see Table V) for coefficients of variation and correlation coefficients using any pair of tested parameter set values from ($S_{vu,C}$, $S_{d20,C}$ and $S_{w,C}$) were at most 1×10^{-34} proving significant difference among means for each tested coupling. The tested correlation coefficients were computed using ($1 + 14 \times 128$) bins (Table V). However, the t-test significance of differences in means is also held for correlation coefficients computed using ($1 + 14 \times 64$) or ($1 + 14 \times 32$) bins in weighted histograms. For S_{d20,C_1} and S_{d1000,C_1} parameter sets (evaluated only for coupling 1), the significance in means of correlation coefficients was not proven (p-value $= 0.686$).

To illustrate the diversity of the existing oscillatory patterns, we present in Fig. 5 a small fraction of obtained oscillating patterns as a result of random sampling of parameters sets ($|T_C| = 1000$) for one selected coupling (Fig. 1(1b)) allowing to gradually changing any connection weight in given coupling. All presented oscillatory behaviour patterns are depicted for selected fixed set of connection delays ($d_{1,\ldots,8} = [32.0, 20.0, 1.0, 30.0, 0.2, 1.5, 0.2, 12.0]$) considering initial setting of all membrane potentials and recovery variables as zero and only non-rare cases are presented. The detailed periodicity patterns for selected parameter sets were then examined and their example is shown in Fig. 6 (see also the examples of accompanied membrane potentials in Supplement Fig. S1).

Supposing that the differences in oscillation patterns can be identified based upon correlation coefficients of their weighted peak interval histograms or similar characteristics, Table VI then shows the detected number of identified oscillation patterns using correlation coefficients of weighted histograms with ($1+14\times128$) bins. When decreasing the sensitivity (using weighted histograms with ($1+14\times64$) or ($1+14\times32$) bins), the drop in detected frequencies also occurs (see Supplement Table S-III, S-IV). The significant changes in peak intervals resulting from small changes in the synaptic weights support

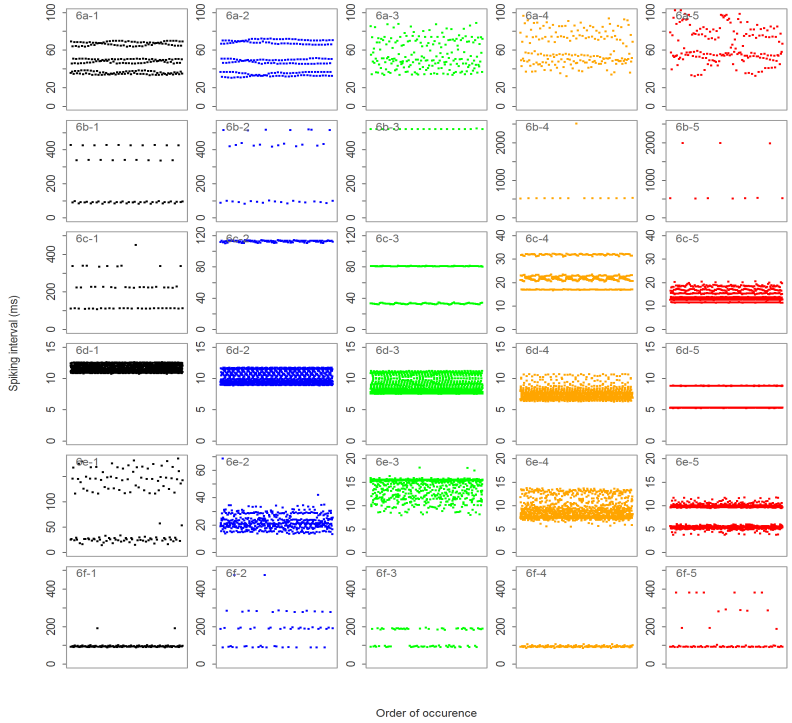

Fig. 6. Periodicity of the time intervals between subsequent peaks. For selected neuron in a coupling with specified weight setting, interneuron connection delay and initial potential and recovery variables setting, the intervals between two sequential peaks were monitored to verify the periodicity of firing patterns behaviour. (6a) the fourth neuron in the coupling with the same settings as in Fig. 3, 3c. Periodicity displayed for weights $w_6 = 2.0, 3.0, 4.0, 5.0, 6.0$, (6b) the fourth neuron in the coupling with the same settings as in Fig. 4, 4b. Periodicity displayed for weights $w_6 = 1.0, 2.0, 3.5, 4.0, 4.5$. For (6c), (6d), (6e), the results are presented for coupling Fig. 1(1b), where individual connection delays $d_{1,\dots,8} = [30.5, 39.0, 12.5, 33.0, 2.5, 4.5, 1.5, 16.5]$ and zero values for initial membrane potentials and recovery variables were considered. (6c) the first neuron in the coupling Fig. 1(1b) with weights set at $w_{1,\dots,8} = [0.5, 5.0, 1.0, 6.5, 2.0, 2.0, 5.0, 2.5]$; periodicity displayed for weights $w_6 = 1.5, 2.0, 3.0, 4.0, 5.0$, (6d) the first neuron in the coupling Fig. 1(1b) with weights set at $w_{1,\dots,8} = [5.0, 1.0, 0.5, 0.5, 0.5, 2.0, 2.5, 6.5]$; periodicity displayed for weights $w_6 = 1.0, 2.0, 3.0, 4.0, 5.0$, (6e) the first neuron in the coupling Fig. 1(1b) with weights set at $w_{1,\dots,8} = [5.0, 2.5, 2.0, 0.5, 5.0, 6.5, 2.0, 2.5]$; periodicity displayed for weights $w_6 = 0.5, 1.0, 3.0, 5.0, 6.5$. (6f) the fifth neuron in the coupling presented in Fig. 1(1c) with the individual connection delays $d_{1,\dots,10} = [33.5, 39.0, 31.0, 19.0, 26.5, 3.0, 24.0, 1.0, 3.0, 1.5]$, synaptic weights set $w_{1,\dots,10} = [2.0, 0.5, 5.0, 2.5, 6.5, 1.0, 0.5, 1.0, 0.5, 2.5]$ and zero values for initial membrane potentials and recovery variables; periodicity displayed for weights $w_{10} = 2.0, 3.0, 3.5, 4.0, 6.0$.

TABLE VI

IDENTIFIED NUMBER OF POSSIBLE DIFFERENT OSCILLATION PATTERNS FOR ALL THREE TESTED COUPLINGS. | T_C |= 100 AND | $S_{w,C}$ |= 100 WERE USED. *THE DETECTED NUMBER OF FREQUENCIES COULD BE ALSO LIMITED BY SAMPLING STEP OF 0.1 nS FOR THE WEIGHTS FROM THE INTERVAL $\langle 0.5, 6.5 \rangle$

Coupling 1 (Fig. 1(1a))					
Max. allowed correlation γ	0.8	0.6	0.4	0.2	0.0
$\mathrm{HiMaxF}_{128,T_C,k_6,S_{w,C}}$	*61	52	43	34	18
$\mathrm{LoMaxF}_{128,T_C,k_6,S_{w,C}}$	*61	49	41	34	17
$\mathrm{LoMinF}_{128,T_C,k_6,S_{w,C}}$	*61	38	19	10	3
Coupling 2 (Fig. 1(1b))					
Max. allowed correlation γ	0.8	0.6	0.4	0.2	0.0
$\mathrm{HiMaxF}_{128,T_C,k_6,S_{w,C}}$	*61	*61	*61	51	28
$\mathrm{LoMaxF}_{128,T_C,k_6,S_{w,C}}$	*61	60	54	40	18
$\mathrm{LoMinF}_{128,T_C,k_6,S_{w,C}}$	*61	57	49	33	16
Coupling 3 (Fig. 1(1c))					
Max. allowed correlation γ	0.8	0.6	0.4	0.2	0.0
$\mathrm{HiMaxF}_{128,T_C,k_6,S_{w,C}}$	*61	*61	*61	57	41
$\mathrm{LoMaxF}_{128,T_C,k_6,S_{w,C}}$	*61	56	50	39	27
$\mathrm{LoMinF}_{128,T_C,k_6,S_{w,C}}$	55	40	30	23	14

our hypothesis that the oscillators could maintain their high information storage capacity because of the availability of many 'intrinsic frequencies' for synchronization.

IV. DISCUSSION

According to our simulations, selected neuronal couplings are able to produce a variety of different behavioural patterns, with peak intervals ranging from milliseconds to thousands of milliseconds between the spikes. The behaviour of these couplings strongly depends on the extent of the excitatory or inhibitory connections between neurons. Modifying these connections, especially by changing the synaptic weight, substantially changes the signal properties of the studied oscillator. Conversely, the dependence on the initial membrane potentials or connection delays seems to be much weaker allowing some level of robustness when recovering the activity after unfavourable conditions or when connections to far neurons are present.

Depending on the structure, the subtype of the coupled neurons, and the connection weights, information could be stored by the oscillatory activity of cortical oscillators in a robust way; if we accept this possibility, the model displays a high number of frequencies for each particular oscillator type. When single neuron in brain receives potential from roughly 10,000 synapses [40], the average synaptic weight in a group of neurons increases as the number of connections increases and quickly saturates well before the maximum

number of interactions is reached [27]. This challenges the original Hebb's postulate of learning [41], where the continuous strengthening of the selected synapses connecting neurons with similar spiking behaviour could easily reach the biological limits. When the synaptic plasticity could enhance the spike-frequency adaptation in pyramidal neurons and consequently affect the synchronization properties of cortical oscillators [42], then there would not be important the absolute conductance of the connection, but only its relative strength in comparison to other connections. High-frequency oscillatory activity in a relatively uniform coupling pattern with a limited number of cortical neuronal subtypes, as supposed by Edelman's theory of Neuronal Group Selection [43], then supports suitability of such oscillating units to encode many different states. In other theories, like Memories as Bifurcations theory [3] or theory of Polychronous patterns and Polychronous Neuronal Groups [14]–[16], coding information as oscillating patterns is also supported and simultaneous presence of several higher-level memories at the same time is proposed. The mechanisms of identical or generalized synchronization then could probably explain reasoning in such networks (see for example [44], [45]) followed by learning methods similar to any weight modification method like spike timing dependent plasticity (STDP) [46] succesfully used in artificial SNN models for pattern recognition [47], [48].

When accepting the idea of reasoning in the brain based on the generalized synchronization principle of connected oscillators, which means that the brain attempts to lower its energy consumption by slightly changing the oscillatory activity patterns and synchronizing the disharmonic oscillations, our results fit well if these synchronizations ultimately lead to changes in synaptic weights.

V. Conclusion

The oscillatory activity of a selected, histologically verified set of neuron couplings modelled by a set of differential equations with parameters within their biological limits showed the complex behavioural patterns significantly depending on the modelled connection weights (conductance) to other oscillating units but relatively weakly depending on the initial membrane potentials or interneuron connection delays. The non-rare occurrence of proper interneuron connection weight settings in an oscillatory group with a potentially large number of intrinsic frequencies in their oscillatory activity supports the idea of possibly large informational capacity of such a neuronal coupling oscillator serving as a basic memory unit.

References

[1] E. M. Izhikevich, "Polychronization: Computation with spikes," *Neural Comput.*, vol. 18, no. 2, pp. 245–282, 2006.

[2] R. Kurzweil and C. Lane, *How to Create a Mind: The Secret of Human Thought Revealed*. Baltimore, MD, USA: Penguin, 2012.

[3] T. Kurikawa and K. Kaneko, "Memories as bifurcations: Realization by collective dynamics of spiking neurons under stochastic inputs," *Neural Netw.*, vol. 62, pp. 25–31, Feb. 2015.

[4] D. J. Amit, *Modeling Brain Function: The World of Attractor Neural Networks*. Cambridge, U.K.: Cambridge Univ. Press, 1992.

[5] W. Maass, "Networks of spiking neurons: The third generation of neural network models," *Neural Netw.*, vol. 10, no. 9, pp. 1659–1671, 1997.

[6] K. J. Friston, "The labile brain. I. Neuronal transients and nonlinear coupling," *Philos. Trans. Roy. Soc. London B, Biol. Sci.*, vol. 355, no. 1394, pp. 215–236, 2000.

[7] T. J. Sejnowski and O. Paulsen, "Network oscillations: Emerging computational principles," *J. Neurosci.*, vol. 26, no. 6, pp. 1673–1676, 2006.

[8] E. M. Izhikevich, T. J. Sejnowski, and T. A. Poggio, *Dynamical Systems in Neuroscience: The Geometry of Excitability and Bursting* (Computational Neuroscience Series). Cambridge, MA, USA: MIT Press, 2006.

[9] K. Nakada, K. Suzuki, and T. Nakada, "Single to two cluster state transition of primary motor cortex 4-posterior (MI-4p) activities in humans," *Entropy*, vol. 17, no. 11, pp. 7596–7607, 2015.

[10] E. L. Ardiel and C. H. Rankin, "An elegant mind: Learning and memory in *Caenorhabditis elegans*," *Learn. Memory*, vol. 17, no. 4, pp. 201–291, 2010.

[11] G. M. Stein and C. Y. Murphy, "*C. Elegans* positive olfactory associative memory is a molecularly conserved behavioral paradigm," *Neurobiol. Learn. Memor*, vol. 115, pp. 86–94, Nov. 2014.

[12] G. S. Duane, "Synchronicity from synchronized chaos," *Entropy*, vol. 17, no. 4, pp. 1701–1733, 2015.

[13] A. L. Shilnikov and N. F. Rulkov, "Origin of chaos in a two-dimensional map modeling spiking-bursting neural activity," *Int. J. Bifurcation Chaos*, vol. 13, no. 11, pp. 3325–3340, 2003.

[14] B. Szatmáry and E. M. Izhikevich, "Spike-timing theory of working memory," *PLoS Comput. Biol.*, vol. 6, no. 8, pp. e1000879-1–e1000879-11, 2010.

[15] P. Ioannou, M. Casey, and A. Grüning, "Factors influencing polychronous group sustainability as a model of working memory," in *Proc. IEEE 24th Int. Conf. Artif. Neural Netw. (ICANN)*, Sep. 2014, pp. 723–731.

[16] P. Ioannou, M. Casey, and A. Grüning, "Spike-timing neuronal modelling of forgetting in immediate serial recall," in *Proc. IEEE Int. Joint Conf. Neural Netw. (IJCNN)*, Jul. 2015, pp. 1–8.

[17] E. M. Izhikevich, "Which model to use for cortical spiking neurons?" *IEEE Trans. Neural Netw.*, vol. 15, no. 5, pp. 1063–1070, Sep. 2004.

[18] P. Ashwin, S. Coombes, and R. Nicks, "Mathematical frameworks for oscillatory network dynamics in neuroscience," *J. Math. Neurosci.*, vol. 6, p. 2, Dec. 2016.

[19] E. M. Izhikevich, "Simple model of spiking neurons," *IEEE Trans. Neural Netw.*, vol. 14, no. 6, pp. 1569–1572, Nov. 2003.

[20] B. Ibarz, J. M. Casado, and M. Sanjuan, "Map-based models in neuronal dynamics," *Phys. Rep.*, vol. 501, nos. 1–2, pp. 1–74, 2011.

[21] E. M. Izhikevich and G. M. Edelman, "Large-scale model of mammalian thalamocortical systems," *Proc. Nat. Acad. Sci. USA*, vol. 105, no. 9, pp. 3593–3598, 2008.

[22] Q. Liu, "Deep spiking neural networks," Ph.D. dissertation, Fac. Sci. Eng., School Comput. Sci., Univ. Manchester, Manchester, U.K. 2018.

[23] S. Chaturvedi, N. R. Sondhiya, R. Titre, A. A. Khurshid, and S. S. Dorle, "Comparison of LIF and Izhikevich spiking neural models for recognition of uppercase and lowercase english characters," *CiiT Int. J. Digit. Image Process.*, vol. 6, no. 6, pp. 276–282, 2014.

[24] A. A. Snaina and R. Abdullah, "Spiking neuron models: A review," *Int. J. Digit. Content Technol. Appl.*, vol. 8, no. 3, pp. 14–21, 2014.

[25] B. W. Connors and M. J. Gutnick, "Intrinsic firing patterns of diverse neocortical neurons," *Trends Neurosci.*, vol. 13, no. 3, pp. 99–104, Mar. 1990.

[26] M. Beierlein, J. R. Gibson, and B. W. Connors, "Two dynamically distinct inhibitory networks in layer 4 of the neocortex," *J. Neurophysiol.*, vol. 90, no. 5, pp. 2987–3000, 2003.

[27] R. Perin, T. K. Berger, and H. Markram, "A synaptic organizing principle for cortical neuronal groups," *Proc. Nat. Acad. Sci. USA*, vol. 108, no. 13, pp. 5419–5424, 2011.

[28] V. Braitenberg and A. Schütz, *Anatomy of the Cortex*. Berlin, Germany: Springer-Verlag, 1991.

[29] W. Gerstner, A. K. Kreiter, H. Markram, and A. V. Herz, "Neural codes: Firing rates and beyond," *Proc. Nat. Acad. Sci. USA*, vol. 94, no. 24, pp. 12740–12741, 1997.

[30] A. K. Kreiter and W. Singer, "On the role of neural synchrony in the primate visual cortex," in *Brain Theory*, A. Aertsen and V. Braitenberg, Eds. Amsterdam, The Netherlands: Elsevier, 1996, pp. 201–227.

[31] W. Singer and C. M. Gray, "Visual feature integration and the temporal correlation hypothesis," *Annu. Rev. Neurosci.*, vol. 18, no. 1, pp. 555–586, 1995.

[32] H. A. Swadlow, "Physiological properties of individual cerebral axons studied *in vivo* for as long as one year," *J. Neurophysiol.*, vol. 54, no. 5, pp. 1346–1362, 1995.

[33] H. A. Swadlow, "Monitoring the excitability of neocortical efferent neurons to direct activation by extracellular current pulses," *J. Neurophysiol.*, vol. 68, no. 2, pp. 605–619, 1992.
[34] D. Wang, "On connectedness: A solution based on oscillatory correlation," *Neural Comput.*, vol. 12, no. 1, pp. 131–139, Jan. 2000.
[35] N. Brunel, F. S. Chance, N. Fourcaud, and L. F. Abbott, "Effects of synaptic noise and filtering on the frequency response of spiking neurons," *Phys. Rev. Lett.*, vol. 86, no. 10, pp. 2186–2189, 2001.
[36] T. Nowotny, R. Huerta, H. D. Abarbanel, and M. I. Rabinovich, "Self-organization in the olfactory system: One shot odor recognition in insects," *Biol. Cybern.*, vol. 93, no. 6, pp. 436–446, 2005.
[37] E. Izhikevich, "Hybrid spiking models," *Philos. Trans. Roy. Soc. A, Math., Phys. Eng. Sci.*, vol. 368, no. 1930, pp. 5061–5070, 2010.
[38] A. C. Hindmarsh, "LSODE and LSODI, two new initial value ordinary differnetial equation solvers," *ACM SIGNUM Newslett.*, vol. 15, no. 4, pp. 10–11, 1980.
[39] R. R. Sokal and F. J. Rohlf, *Biometry: The Principles and Practices of Statistics in Biological Research*. New York, NY, USA: W. H. Freeman and Company, 1995.
[40] W. Maass, "Computing with spikes," *Special Issue Found. Inf. Process. TELEMATIK*, vol. 8, no. 1, pp. 32–36, 2002.
[41] D. O. Hebb, *The Organization of Behavior: A Neuropsychological Theory*. New York, NY, USA: Wiley, 1949.
[42] S. M. Crook, G. B. Ermentrout, and J. M. Bower, "Spike frequency adaptation affects the synchronization properties of networks of cortical oscillations," *Neural Comput.*, vol. 10, no. 4, pp. 837–854, 1998.
[43] G. Edelman, *Neural Darwinism: The Theory Of Neuronal Group Selection*. Oxford, U.K.: Oxford Univ. Press, 1989.
[44] T. E. Akam and D. M. Kullmann, "Efficient 'communication through coherence' requires oscillations structured to minimize interference between signals," *PLoS Comput. Biol.*, vol. 8, no. 11, p. e1002760, 2012.
[45] J. M. Gonzáles-Miranda, *Synchronization and Control of Chaos*. London, U.K.: Imperial College Press, 2004.
[46] H. Markram, W. Gerstner, and P. Sjöström, "Spike-timing-dependent plasticity: A comprehensive overview," *Frontiers Synaptic Neurosci.*, vol. 4, no. 2, pp. 1–3, 2012.
[47] P. Diehl and M. Cook, "Unsupervised learning of digit recognition using spike-timing-dependent plasticity," *Frontiers Comput. Neurosci.*, vol. 9, no. 99, pp. 1–9, 2015.
[48] M. Mozafari, S. Kheradpisheh, T. Masquelier, A. Nowzari-Dalini, and M. Ganjtabesh, "First-spike based visual categorization using reward-modulated STDP," *IEEE Trans. Neural Netw. Learn. Syst.*, vol. 29, no. 12, pp. 6178–6190, 2018.